



Usage of fruit-fibers of *Luffa cylindrica* for the sorptive removal of Direct Blue 15 dye from water

Abdul Rauf^{a,*}, Tariq Mahmud^a, Muhammad Ashraf^b, Rabia Rehman^a, Sumaira Basharat^a

^aUniversity of the Punjab, Quaid-e-Azam campus, Lahore, Pakistan, Tel. +923214752437, email: abdurraouf07@gmail.com (A. Rauf), Tel. +923334206465, email: tariqbutt.chem@pu.edu.pk (T. Mahmud), Tel. +92-42-99230463 Ext# 870, email: grinorganic@yahoo.com (R. Rehman), Tel. +923366123478, email: samrabasharat@gmail.com (S. Basharat)

^bPCSIR Laboratories, Lahore, Pakistan, Tel. +923004196021, email: drashrafchaudhry@yahoo.com (M. Ashraf)

Received 20 October 2017; Accepted 1 July 2018

ABSTRACT

Biosorption is a cheaper process to remove heavy metal ions and dyes from waste water. In this study untreated and alkali treated fruit-fibers of *Luffa cylindrica* sponge have been used to remove Direct Blue 15 dye from water. This dye is carcinogenic in nature. Alkali treatment was given in view of the mercerization process to increase the dye-removal efficiency of the fibers. Different optimization parameters were studied such as pH 2, rotational speed 125 rpm, initial dye concentration 20 ppm, biosorbent dosage 0.3 g and temperature 60 °C. Isothermal studies showed that the Langmuir model was the best fit isotherm. The maximum adsorption capacity was 9.75 mg/g with alkali treated fibers as compared to 8.05 mg/g with the untreated fibers. Kinetic studies showed that Ho's model was more applicable. The mechanism was mainly the film diffusion along with the intraparticle diffusion. Thermal studies signified that the adsorption of the dye was a spontaneous and exothermic process but also suggested it as physisorption as compared to chemisorption deduced from the kinetic studies. FTIR studies identified hydroxyl and carboxyl functional groups responsible for the adsorption of the dye.

Keywords: Mercerization; Langmuir isotherm; Ho's model; Film diffusion; Physisorption

1. Introduction

The dyes are those pollutants which come into visual water pollution. There are about 10,000 different dyes which are being synthesized and used in textile, paper, leather, pharmaceutical, food and other industries. The annual production of these dyes is about 7×10^5 metric tons. The textile industry is the main source of water pollution as about 200,000 tons of these dyes go unused in the environment due to flaws in the dyeing procedures [1,2]. These dyes are responsible for the aesthetic value of water. These molecules cause an increase in COD (Chemical oxygen demand) and BOD (Biological oxygen demand) values of water due

to increase in consumption of dissolved oxygen in water for the oxidation of such types of molecules. This in turn threatens the aquatic life by reducing the available oxygen in water [3,4]. The process of photosynthesis is more affected by these dyes as compared to the invisible pollution because the sun light cannot easily transmit through the water. Some types of the dyes such as azo dyes are also carcinogenic in nature.

Dyes have been classified according to their applications, structures etc. The Direct dyes are soluble in aqueous media due to sulfonic, amino or any other ionic interaction. These dyes are benzidine based which make them potentially carcinogenic in nature, so these dyes or their metabolites cause serious threat to the living organisms [5,6]. The spent dye solutions are discharged into the environment

*Corresponding author.

without processing in most of the countries. These dyes are also resistant to natural degradation as these dyes are synthesized with an aim to make them resistant to degradation, higher fastness and brilliance [7].

There are many processes which are being used to treat the polluted waters before they are discharged to the natural waters. These include filtration, precipitation, oxidation reduction, membrane technologies, ozonation, color irradiation etc. But these processes are costly and not so efficient in removal of the pollutants [8]. These processes may also be not eco-friendly due to formation of sludge and other waste material. Although charcoal has also been used for absorbing the dyestuff, but due to higher cost, its use is limiting [9]. In the recent years much research work has been done on the biosorption process to discover new more efficient biosorbent materials to tackle the problem of water pollution. The process is cheaper and eco-friendly. In this process live or dead plant or any other species' material is used for the sorption of contaminants from water [10,11]. Dead plant material is easily available in the form of agricultural waste material and is not affected by the hazardous chemicals, so it has major significance in removal of dyes and heavy metal ions. The main mechanisms involved in biosorption are: particle diffusion, ion exchange and physical forces [12]. The plant based dead biomass such as saw dust [13], wheat bran [14], rice husk [15], cotton stalk [16], spent tea leaves [17], orange peels [18], pine needles [19], sugarcane bagasse [20], peanut hull [21], coconut husk [22], other lignocellulosic materials etc. have been used in recent years to study the biosorption of dyes and heavy metal ions.

In present work we have used untreated (UnT) and alkali treated (AT) fruit-fibers of *Luffa cylindrica* (FFLC) for the sorptive removal of Direct Blue 15 (DB 15) dye from the aqueous media. Previously we used spent tea leaves and papaya leaves for the removal of Direct Blue 15 dye [17]. But *Luffa cylindrica* showed much more efficiency in removal of DB 15 dye as compared to the spent tea leaves and papaya leaves. The aim of this work was to give alkali treatment similar to mercerization process for increasing the dye-removal efficiency of the FFLC. Alkali treatment makes the cellulosic fibers more adhesive to the dyes by changing their morphology.

Luffa cylindrica is a subtropical plant which belongs to Cucurbitaceae family. It is cultivated in warm regions of Asia such as Pakistan, India, Vietnam, Korea, Central America and in some regions of Africa. Its common names are bath sponge, dish-cloth gourd, sponge gourd etc. Its fruit has oblong cylindrical shape, having extended fibrous network core with a spongy mat like structure (Fig. 1). This is in fact xylem which contains the seeds of the fruit in a specific arrangement. The fibers are made up of 60% cellulose, 30% hemicelluloses and 10% lignin [23].

Luffa cylindrica has been used in various research fields such as in composite materials due to its morphological and mechanical properties, medicine and in biosorption of dyes and heavy metal ions. It has been used for the biosorptive removal of Methylene blue [9,24], Malachite green [25], Brilliant green [26] and Alizarin Yellow-R [27] dyes. It has also been used as an immobilized surface for *Phanerochaete chrysosporium*, *Funalia tolgii*, *Proteus vulgaris* NCIM-2027 for



Fig. 1. Dried fruit of *Luffa cylindrica*.

decolourization of Remazol Brilliant Blue R [28], Reactive Black 5 [29] and Reactive blue 172 [30] respectively. It has also been used to remove nickel, copper, zinc, lead and cadmium ions from the aqueous media [31–33].

Direct Blue 15 is an azo class dye with CI No. 24400 (Fig. 2). Its molecular formula is $C_{34}H_{24}N_6Na_4O_{16}S_4$ and molar mass is 992.80 g/mol. Its other names are: Direct Sky Blue, Sky Blue 5B, Direct Torquiose Blue, Sky Blue FB, Nippon Sky Blue, Niagara Sky Blue etc. It was firstly produced in 1890 [34,35]. It is employed for dyeing cellulose, leather, cotton, paper, wool, silk and in staining biological matter. It is soluble in water making dark blue color solution but insoluble in organic solvents. It can be anaerobically biodegraded to 3,3'-dimethoxybenzidine in polluted waters which is classified as group 2A carcinogenic compound [36]. The starting material of the dye at the manufacturing site is lethal to the living organisms due to its air borne nature. So, the dye should be handled with care and its entrance to the environment should be checked seriously.

2. Materials and methods

2.1. Preparation of the biosorbent

The dried sponges of *Luffa cylindrica* were purchased from the local market of Lahore and home grown sponges were also used. The sponges were peeled off and internal fibrous body was cut into pieces. These pieces were washed, dried and cut into smaller pieces. They were pulverized in the grinder and separated into 20, 40, 60 and 80 mesh sizes. The fibers were then immersed in 0.1 M NaOH solution and stirred for an hour at 100 rpm speed. The caustic soda solution caused the removal of lignin from the xylem body and changed the surface morphology of the fibers. The alkali treated fibers were rinsed with distilled water and dried in oven at 80 °C. They were stored in air tight bottles and labeled as FFLC. 40 mesh size fibers were used in the biosorption experiments.

2.2. Preparation of standard solutions of the dye

Direct Blue 15 dye was purchased from Shanghai Chemicals, China. It was used as such. The standard solutions of 5 ppm to 25 ppm were made for instrument calibration. For this purpose absorbance values were determined by using

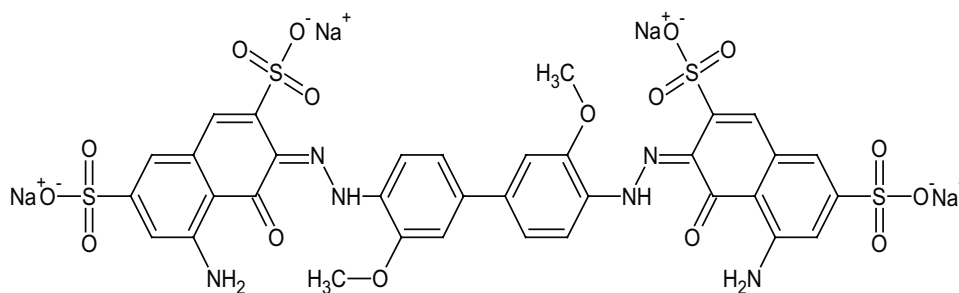


Fig. 2. Direct Blue 15 molecular structure.

China Visible Spectrophotometer 720 at λ_{\max} 603 nm. The pH meter (Hanna), orbital shaker (Sky Line Analog) and FTIR spectrometer (Agilent Cary 630) were used in this work.

2.3. Batch wise experiments

Batchwise experiments were conducted by varying the experimental conditions such as initial dye concentration, biosorbent dosage, rotational speed, pH and temperature. In this study both the alkali treated and untreated FFLC were used to evaluate the effect of chemical treatment on the biosorption efficiency. Isothermal, kinetic and thermal studies were also conducted. The experiments were repeated and error bars were shown in the graphs.

The formulae which were used to determine the percentage removal and study isothermal, kinetic and thermodynamic factors are given below in Eqs.(1) and (2).

$$\text{Removal (\%)} \text{ of the dye} = \frac{C_i - C_e}{C_i} \times 100 \quad (1)$$

$$Q_e = \frac{(C_i - C_e)V}{m} \quad (2)$$

Here C_i is initial concentration of DB15 dye in ppm, C_e is the remaining concentration in the solution, Q_e is the amount of the dye adsorbed in mg/g on the biosorbent, 'm' is FFLC amount in grams and V is the volume of the solution in litre.

3. Results and discussion

FTIR analysis showed the presence of functional groups such as carboxyl, hydroxyl etc. The peak at 3333 cm^{-1} corresponded to OH stretching vibration which slightly decreased to 3332 cm^{-1} after the dye adsorption. The peak at 2895 cm^{-1} corresponded to CH_2 and CH_3 stretching vibrations which changed to 2880 cm^{-1} after adsorption. The peak at 1655 cm^{-1} signified the bending vibration of the adsorbed water which slightly decreased to 1653 cm^{-1} after the biosorption. The aromatic ring related to lignin at 1508 cm^{-1} disappeared in DB 15 dye-adsorbed fibers of *Luffa cylindrica*, CH_2 and CH_3 bending vibrations were located at 1421 cm^{-1} , while CH bending vibration appeared at 1320 cm^{-1} , C-O-C bending vibration in cellulose and hemicellulose at 1195 cm^{-1} decreased to 1159 cm^{-1} after the dye adsorption, C-OR (Cellulose) stretching vibration at 1026 cm^{-1} was increased to 1029 cm^{-1} . The

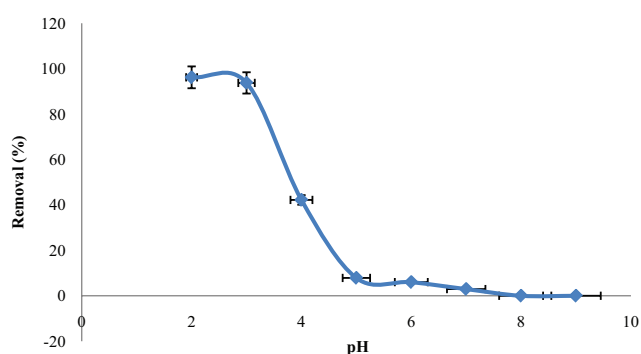


Fig. 3. Effect of pH on removal (%) of DB 15 dye by alkali treated FFLC.

peak corresponding to β -glucosidic linkage at 898 cm^{-1} was decreased to 896 cm^{-1} after adsorption [25,37].

3.1. Optimization parameters

The effects of different parameters were studied to get their optimum values for the biosorptive removal of DB 15 dye. The optimum pH value was 2.0 where 96.19% of DB 15 dye was removed but with increase in pH the biosorption efficiency was decreased (Fig. 3). It revealed that at lower pH the surface of the biosorbent was protonated which helped in binding the DB15 dye molecules to the surface of the biosorbent through ionic interactions and hydrogen bonding. At higher pH due to repulsive negative forces, the dye molecules could not attach to the surface of the fibers and hence no efficient biosorption happened. At the agitation speed of 125 rpm the maximum uptake was 94.96% (Fig. 4). This showed that with increase in the speed of agitation, the number of collisions among the biosorbent and the dye molecules increased and resulted in greater removal of the dye. At lower speeds, there were no sufficient contacts among the biosorbent and the dye molecules which could result in greater removal. Biosorbent dosage of 0.3 g showed maximum removal of 96.07% with 50 ppm dye solution (Fig. 5). It was noticed that with increase in amount of the biosorbent, the surface area increased and hence more the active sites were available for binding to the dye molecules. The study of temperature effect revealed that percentage removal increased with increase in temperature. Higher temperatures provided more kinetic energy to

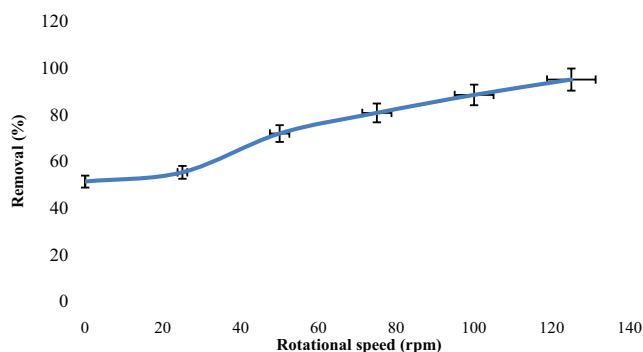


Fig. 4. Effect of rotational speed on removal (%) of DB 15 dye by alkali treated FFLC.

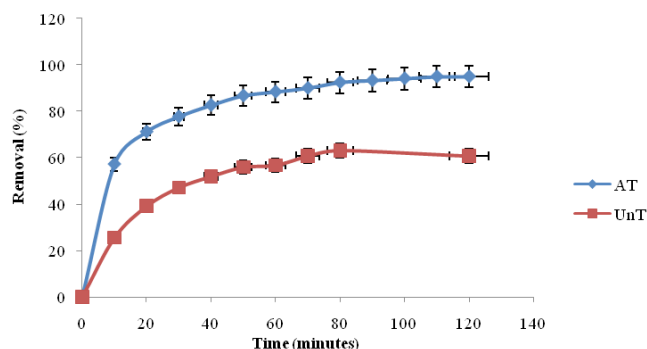


Fig. 7. Effect of contact time on removal (%) of DB 15 dye by AT and UnT FFLC.

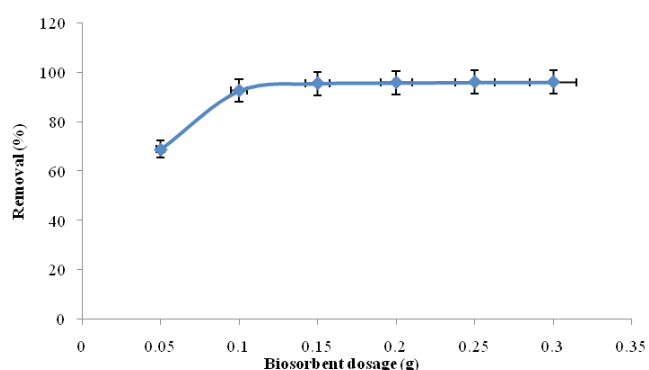


Fig. 5. Effect of biosorbent dosage on removal (%) of DB 15 dye by alkali treated FFLC.

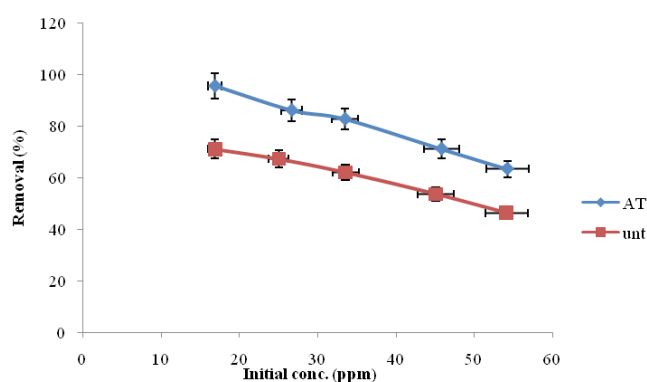


Fig. 8. Effect of initial conc. of the dye on removal (%) of DB 15 dye by AT and UnT FFLC.

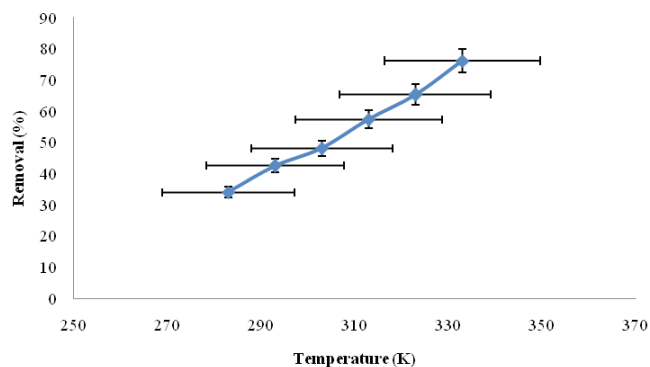


Fig. 6. Effect of temperature on removal (%) of DB 15 dye by alkali treated FFLC.

the molecules for interaction with the active sites and overcome the activation energy barriers. Maximum removal was 76.09% at 60 °C with gentle shaking for 5 min with 0.05 g of the biosorbent in 10 ppm solution (Fig. 6). It took about 2 h of contact time with 94.93% removal with alkali treated fibers and 63.09% with the untreated fibers to establish the equilibrium at the optimum conditions (Fig. 7). At 20 ppm initial dye concentration, percentage removal was 95.63% and 71.22% with the alkali treated and the untreated fibers respectively (Fig. 8). With increase in the concentration of the dye, percentage removal decreased due to decrease in the active sites available for the adsorption.

3.2. Isothermal studies

When the dye solution and the biosorbent are kept for a longer time at a constant temperature then equilibrium is established between sorption and desorption and the studies done are called the isothermal studies. A graph was plotted between Q_e and C_e using different initial concentrations of the dye, showing achievement of the equilibrium (Fig. 9). Different isothermal models such as linear forms of Langmuir [38], Freundlich [39], Temkin [40] and Dubinin-Radushkevich [41,42] were applied to the equilibrium data.

The Langmuir model has theoretical bases. This model considers the monolayer coverage on a homogeneous surface with no association among the adsorbed species. Mathematically Langmuir isotherm can be written in linear form as shown in Eq. (3):

$$\frac{1}{Q_e} = \frac{1}{K_L Q_m C_e} + \frac{1}{Q_m} \quad (3)$$

Here Q_e represents the quantity of DB 15 dye adsorbed at equilibrium in mg/g, Q_m is the maximum amount of DB 15 dye adsorbed on FFLC surface and K_L represents the Langmuir constant which is used to determine the value of separation factor R_L as shown in Eq. (4). The separation factor R_L is important in isothermal studies, as knowing the value of R_L , we can predict the favorability of the adsorption process. If $R_L = 0$ then the biosorption process is irreversible,

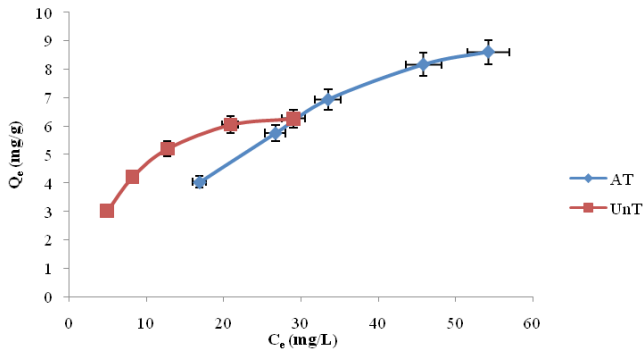


Fig. 9. Graph between C_e and Q_e values of DB 15 dye removed by AT and UnT FFLC.

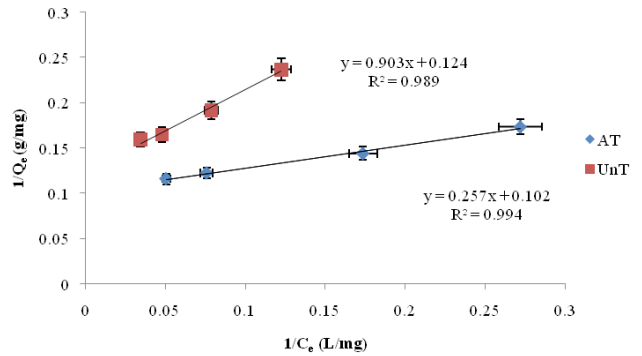


Fig. 10. Langmuir isotherms for the adsorption of DB 15 dye by AT and UnT FFLC.

if $0 < R_L < 1$ then the process is favorable, if $R_L > 1$ then it is unfavourable and if $R_L = 1$ then it is linear [43].

$$R_L = \frac{1}{1 + K_L C_i} \quad (4)$$

Here C_i is the initial concentration of the dye. Fig. 10 shows the Langmuir isotherms for the alkali treated and the untreated FFLC for the removal of DB 15 dye.

The Freundlich isotherm which is a case of Langmuir isotherm is related to adsorption on heterogeneous surfaces. It has empirical bases instead of theoretical as in case of Langmuir isotherm. This model can be shown mathematically as in Eq. (5).

$$\log Q_e = \log K_F + \frac{1}{n} \log C_e \quad (5)$$

In this equation Q_e represents the quantity of DB 15 dye adsorbed on FFLC surface in mg/g at equilibrium. K_F and n are Freundlich constants. The value of n is important as it tells the adsorption efficiency and heterogeneity of the surface. The value of $1/n$ ranges from 0 to 1, an n value greater than 1 but less than 10 is considered good for the adsorption process [44]. K_F is the relative adsorptivity which is linked to the amount of the dye adsorbed on the surface of the biosorbent at the equilibrium. This isotherm is applicable at moderate concentrations of the dye but at higher concentrations it is not pertinent. Fig. 11 shows the Freundlich isotherms for the alkali treated and the untreated FFLC.

Temkin isotherm is related to the heat of adsorption. This model assumes that the heat of adsorption decreases linearly with increase in adsorption coverage. It also says that the binding energies are uniformly distributed on the surface reaching up to a maximum value [45]. The linearized form of the Temkin isotherm can be shown as in Eq. (6).

$$Q_e = B \ln A + B \ln C_e \quad (6)$$

where $B = \frac{RT}{b}$ (7)

Here Q_e is the amount of the dye adsorbed at the equilibrium, B and b are the Temkin constants linked to the heat of adsorption, A is the equilibrium binding constant related to the maximum binding energy, R is the general gas con-

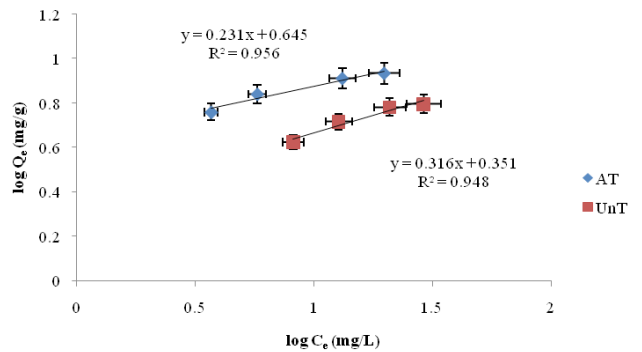


Fig. 11. Freundlich isotherms for the adsorption of DB 15 dye on AT and UnT FFLC.

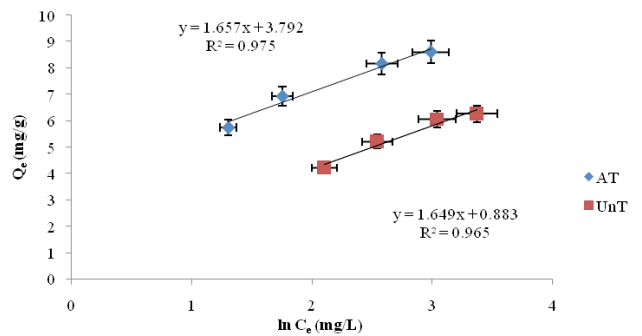


Fig. 12. Temkin isotherms for the adsorption of DB 15 dye by AT and UnT FFLC.

stant and T is the room temperature. Fig. 12 shows the Temkin isotherms for the adsorption of DB 15 dye on the alkali treated and the untreated FFLC.

Dubinin-Radushkevich (DR) isotherm is related to the particular porosity of the biosorbent and the adsorption energy as shown in Eqs. (8), (9) and (10) [46,47].

$$\ln Q_e = \ln Q_m - 2B_D \varepsilon^2 \quad (8)$$

where $\varepsilon = RT \ln \left(1 + \frac{1}{C_e} \right)$ (9)

Here Q_e is the quantity of DB 15 dye adsorbed on the surface of the biosorbent, C_e is the equilibrium concentration of the dye in solution, Q_m is the Dubinin-Radushkevich constant linked to the degree of adsorption. B_D is the free energy of the dye molecules per mole which migrate from an infinite distance to the surface of the fiber and ϵ is Polanyi potential. The apparent energy of adsorption E_D can be calculated by using the value of B_D as shown in Eq. (10). Fig. 13 shows the DR isotherms for the adsorption of DB 15 dye on the alkali treated and the untreated FFLC.

$$E_D = \sqrt{(1 / 2B_D)} \quad (10)$$

Value of E can give valuable information about the adsorption mechanism, if $E < 8$ KJ/mol then the mechanism may be physical adsorption, if it is $8 < E < 16$ KJ/mol, then ion exchange and if $E > 16$ KJ/mol, then it can be chemical adsorption. In this work, value of E in both the cases was less than 8 KJ/mol which indicated physical adsorption of the dye [48].

Table 1 shows the values of different isothermal parameters applied in these studies. It has been found that the Langmuir isotherm is more applicable as compared to any other isotherm evident from its R^2 value.

3.3. Kinetic studies

Various kinetic models have been used to study the mechanism of biosorption process and the steps involved in controlling the rate of sorption because it is important in designing and selecting the optimum conditions for pilot scale system. Some of these models include the pseudo first order or Lagergren model [49], the pseudo second order or Ho's model [50] and Elovich model [51]. 0.1 g each of alkali treated and untreated FFLC was used with 10 ppm dye solution at optimum values of pH and agitation speed at room temperature. A graph was plotted between time t in minutes and Q_t , the quantity of the dye adsorbed in mg/g at any time t , till the equilibrium was established as shown in Fig. 14. Initially the rate of adsorption increases rapidly then it becomes constant.

Lagergren was the first to present a model for describing the adsorption rate of oxalic acid and malonic acid on charcoal on the bases of adsorption capacity [50]. The linear form of pseudo first order or Lagergren's equation is shown in Eq. (11).

$$\ln(Q_e - Q_t) \ln(Q_e - Q_i) = \ln Q_e - k_1 t \quad (11)$$

Here Q_e is the quantity of DB 15 dye adsorbed at the equilibrium while Q_t is the amount of the dye adsorbed at any instant. K_1 is the rate constant of pseudo first order and t represents the time in min. Linear plots between $\ln(Q_e - Q_t)$ vs. time t were drawn for the untreated and the alkali treated FFLC used for the removal of DB15 dye. R^2 value was closer to 1.00 in both the cases. Value of K_1 was calculated from the linear equation of the graph. However the calculated value of Q_e was different from the experimental value which showed non applicability of the model. It is also cited in the literature that it is applicable for initial 20–30 min and not for the whole range of contact time [52].

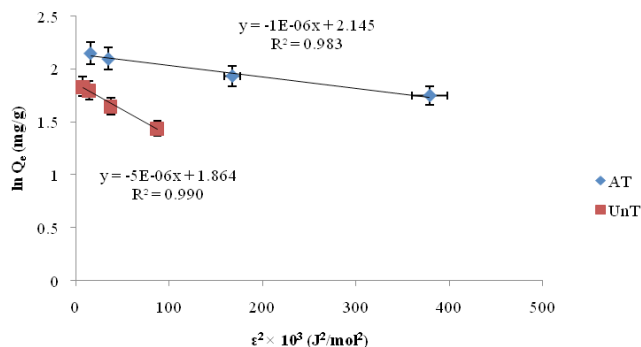


Fig. 13. DR isotherms for the adsorption of DB 15 dye by AT and UnT FFLC.

Table 1
Different isothermal parameters for the adsorption of DB 15 dye on FFLC

Langmuir				
	Q_m (mg/g)	K_L (L/g)	R_L	R^2
Alkali treated	9.75	0.4	0.04–0.08	0.9945
Untreated	8.05	0.14	0.3–0.13	0.9893
Freundlich				
	K_F (mg/g)	n	R^2	
Alkali treated	4.41	4.32	0.9562	
Untreated	2.24	3.16	0.9428	
Temkin				
	A (L/mg)	B (J/mol)	R^2	
Alkali treated	3.79	1.65	0.9751	
Untreated	0.88	1.65	0.9655	
Dubinin-Raduskevich				
	Q_m (mg/g)	B_D (mol ² /KJ ²)	E_D (KJ/mol)	R^2
Alkali treated	8.55	5×10^{-7}	1.0	0.9837
Untreated	6.45	2.5×10^{-6}	0.45	0.9906

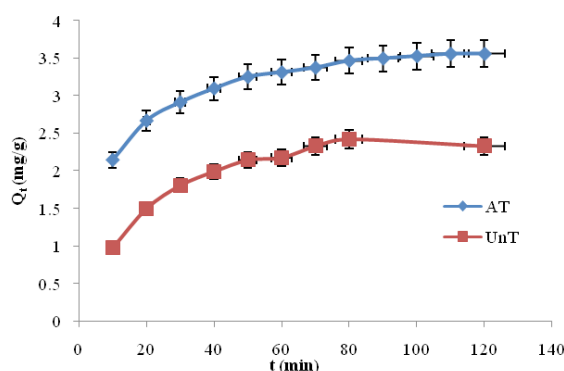


Fig. 14. Graph between t and Q_t for the removal of DB 15 dye by AT and UnT FFLC.

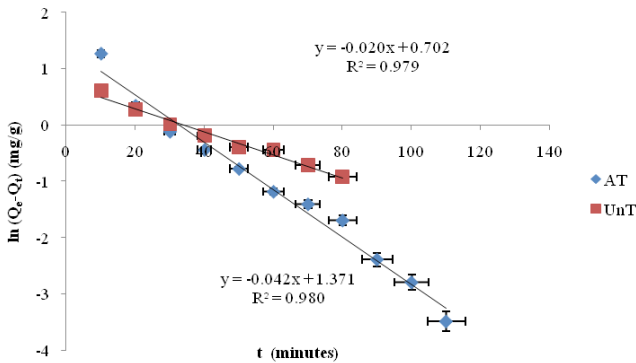


Fig. 15. Pseudo 1st order model for the adsorption of DB 15 dye on AT and UnT FFLC.

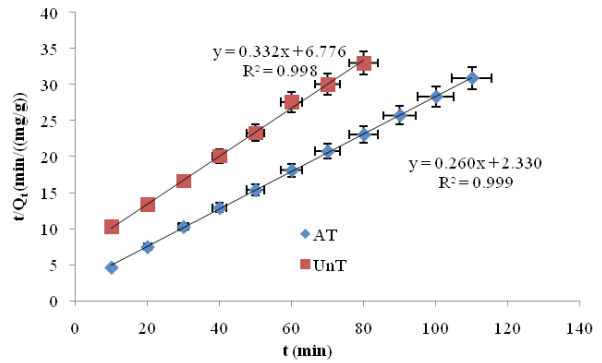


Fig. 16. Pseudo 2nd order model for the adsorption of DB 15 dye on AT and UnT FFLC.

Fig. 15 shows the pseudo first order rates for the adsorption of DB 15 dye on the alkali treated and the untreated FFLC.

In 1995, Ho described the adsorption of divalent ions on the peat surface having various functional groups following pseudo second order rate of reaction. This model is applicable for the whole period of contact time and chemisorption is considered as the rate determining step [50,53]. The linear form is shown in Eq. (12).

$$\frac{t}{Q_t} = \frac{1}{K_2 Q_e^2} + \frac{t}{Q_e} \quad (12)$$

Here Q_e is the quantity of DB 15 dye adsorbed at the equilibrium while Q_t is the amount of the dye adsorbed at any instant. K_2 is the rate constant of pseudo second order and t represents the time in minutes. Linear plots between t/Q_t vs. time t were drawn for untreated and alkali treated biosorbents used for the removal of DB 15 dye. Value of K_2 was calculated from the linear equation of the graph. R^2 value was closer to 1.00 than the Lagergren model in both the cases. The calculated value of Q_e was also closer to the experimental value of Q_e which shows the applicability of this model on the following process. Fig. 16 shows the pseudo second order rates of reactions for the adsorption of DB 15 dye on the alkali treated and the untreated FFLC.

The Elovich model was presented by Chien and Clayton [51] describing the extent of chemisorption mechanism during the sorption process. This model describes second order kinetics with the assumption of heterogeneous surface but it does not describe any explicit mechanism of adsorption [50]. The model is given below as in Eq. (13).

$$Q_t = \frac{1}{\beta} \ln(\alpha\beta) + \frac{1}{\beta} \ln(t) \quad (13)$$

Here Q_t is the amount of the dye adsorbed at any instant. The constant α is linked with the initial adsorption rate and a higher value of α depicts chemisorption. The constant β is linked with the number of active sites, hence the surface coverage [54,55]. Fig. 17 shows the Elovich model for the adsorption of DB 15 on the alkali treated and the untreated FFLC. The R^2 value in both the cases was closer to 1.00. In all three kinetic models applied, the pseudo second order or Ho's model had the closest value to 1.00. So, it is more dominant in this process. The values of different kinetic parameters are shown in Table 2.

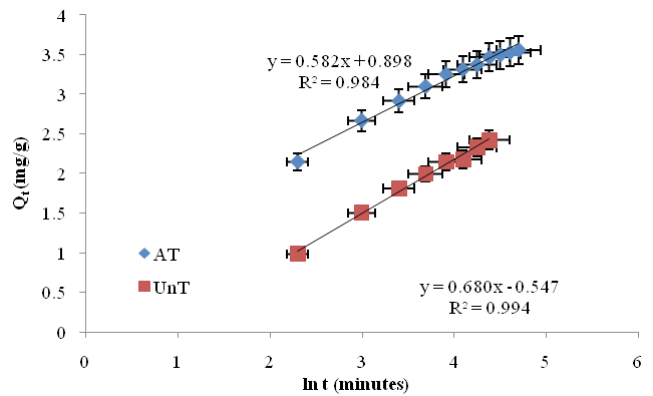


Fig. 17. Elovich model for the adsorption of DB 15 dye on AT and UnT FFLC.

The adsorption mechanism was studied using models of film diffusion [56] and intraparticle diffusion [57]. The process may be controlled by either one or more than one steps including film diffusion, pore diffusion surface diffusion etc. The linear Weber-Morris plot of intraparticle diffusion is shown in Eq. (14).

$$Q_t = K_{ip} t^{1/2} \quad (14)$$

Here Q_t represents the quantity of the dye adsorbed at any instant, K_{ip} is the intraparticle diffusion constant and C represents the thickness of the boundary layer. The plot of Q_t vs. $t^{1/2}$ could be a straight line passing through the origin, if the adsorption process followed the intraparticle diffusion. But it was seen that in both the cases of alkali treated and untreated fibers, the graph was multiline as shown in Fig. 18. This indicated that the process was influenced by two or more steps. The first step was designated as mesoporous diffusion while the second step pointed towards the microporous diffusion [58]. The mesoporous sorption looked faster while the microporous sorption was gradual as shown in Fig. 18. The linear portions did not pass through the origin when extrapolated backwards which indicated that there were other factors also which control the rate of adsorption. The other reason was different rates of mesoporous and microporous diffusion [59]. The value

Table 2
Different kinetic parameters for the adsorption of DB 15dye on FFLC

Pseudo firstorder				
	$Q_{e(Calc.)}$ (mg/g)	$Q_{e(Exp.)}$ (mg/g)	K_1 (1/min)	R^2
Alkali treated	2.66	3.56	0.0074	0.9023
Untreated	1.88	2.42	0.057	0.9792
Pseudo second order				
	$Q_{e(Calc.)}$ (mg/g)	$Q_{e(Exp.)}$ (mg/g)	K_2 (g/(mgmin))	R^2
Alkali treated	3.83	3.56	0.26	0.9997
Untreated	3.00	2.42	0.51	0.9981
Elovich				
	α (g/(mgmin))	β (g/mg)	R^2	
Alkali treated	2.72	1.72	0.9848	
Untreated	1.52	1.47	0.9942	
Intraparticle diffusion				
	C (mg/g)	K_{id} (mg/(gmin ^{1/2}))	R^2	
Alkali treated	1.85	0.18	0.916	
Untreated	0.37	0.24	0.9275	
Film diffusion				
	K_{fd} (1/min)	R^2		
Alkali treated	0.039	0.9826		
Untreated	0.041	0.9676		

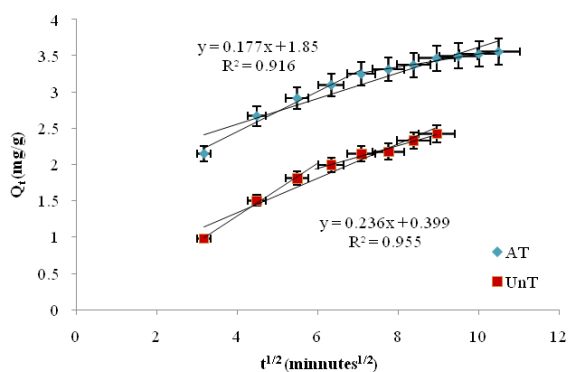


Fig. 18. Intraparticle diffusion model for the adsorption of DB 15 dye on AT and UnT FFLC.

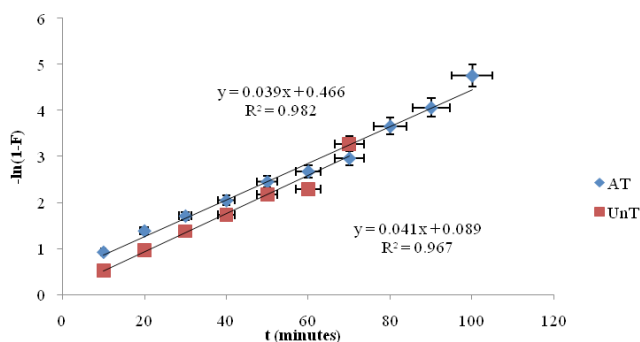


Fig. 19. Film diffusion model for the adsorption of DB 15 dye on AT and UnT FFLC.

of boundary thickness was more significant in case of alkali treated as compared to untreated FFLC.

The film diffusion model, also called Boyd’s model, was applied according to the Eqs. (15) and (16). A linear graph was plotted between $-\ln(1-F)$ and t [56]. Here F is the fractional attainment of equilibrium (Q_t/Q_e). It can be seen in Fig. 19 that the straight line did not pass through the origin which inferred that the film diffusion mechanism was not the sole mechanism of sorption process. This model is similar to pseudo first order or Lagergren model but Boyd’s model depends upon the agitation speed also [60]. It can be seen in Fig. 19 that the film diffusion held at the initial stages but later on it deviated from linearity in the both experiments.

$$\ln(1 - F) = -K_{fd}t \tag{15}$$

$$\text{where } K_{fd} = 3D_e / \Delta rrK \tag{16}$$

Here K_{fd} is the liquid film diffusion constant or external mass transfer constant, D_e is the effective liquid film diffusion constant, r is the radius of the adsorbent bead, Δr is the thickness of the liquid film and K is the equilibrium constant [61,62]. The film diffusion mechanism was more dominant over intraparticle diffusion because the values of the correlation factor (R^2) were closer to unity as compared to intraparticle diffusion. The intercept values were also closer to zero, suggesting that the film diffusion process was more prominent, especially in case of untreated FFLC due to its surface morphology. Table 2 shows the values of parameters of different kinetic models applied in this work.

3.4. Thermodynamic studies

The sorption experiments were done at various temperatures ranging from 10 °C to 70 °C. Fig. 20 shows the Van't Hoff plot for the adsorption of DB 15 dye on alkali treated FFLC. Eqs. (17), (18) and (19) were used to calculate the values of ΔG , ΔH and ΔS (Table 3). These values showed that the sorption of DB 15 dye on FFLC was an exothermic and spontaneous process. It was observed that the value of ΔG increased (become less negative) with increase in temperature up to 60 °C. The value of ΔH was less than 40 KJ/mol and ΔG was also less than 80 KJ/mol which indicated physisorption nature of the adsorption process [63,64]. Although the pseudo second order model predicted it to be chemisorption, the rates are not a good criterion for differentiation between chemisorption and physisorption process [65].

$$\ln K_d = \frac{-\Delta H^\circ}{RT} + \frac{\Delta S^\circ}{R} \quad (17)$$

$$\Delta G^\circ = -RT \ln K_d \quad (18)$$

$$\text{where } K_d = \frac{Q_e}{C_e} \quad (19)$$

4. Conclusions

In present work it has been demonstrated that fruit-fibers of *Luffa cylindrica* become more efficient in removing Direct Blue 15 dye after alkali treatment. Alkali treatment was given in light of mercerization process. FTIR studies approved the presence of hydroxyl and carboxyl functional groups responsible for the attachment of the dye molecules. Isothermal studies showed that Langmuir isotherm was the best fit model among the Freundlich, Temkin and Dubinin Raduskevich isotherms due to higher value of correlation co-efficient. Similarly, in studying rate of reactions, Ho's

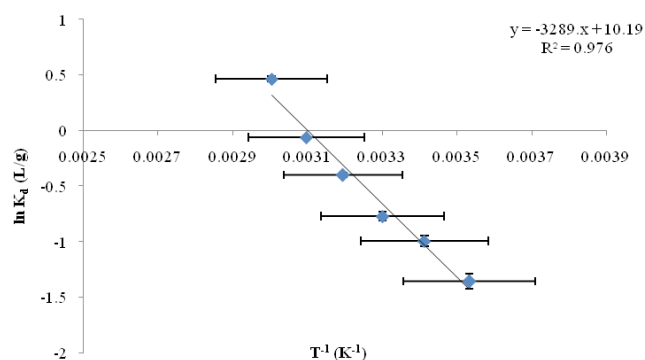


Fig. 20. Arrhenius plot for the adsorption of DB 15 dye on alkali treated FFLC.

Table 3

Different thermal parameters for the adsorption of DB 15 dye on alkali treated FFLC

ΔG (KJ/mol)						ΔH	ΔS
283 K	293 K	303 K	313 K	323 K	333 K	(KJ/mol)	(J/mol K)
-51.3433	-52.1911	-53.0388	-53.8866	-54.7343	-55.5821	-27.352	84.775

model was more applicable as compared to Lagergren and Elovich models due to closer agreement in experimental and model-calculated Q_e values. The main rate controlling mechanism was the film diffusion mechanism as compared to intraparticle diffusion. The thermal studies showed that the process was exothermic and spontaneous in nature as evident from ΔG , ΔH and ΔS values. Previously we used spent tea leaves (1.86 mg/g) and papaya leaves (1.28 mg/g) in removing DB 15 dye but FFLC proved to be more efficient biosorbent (UnT: 8.05 mg/g and AT: 9.75 mg/g). The DR equation and thermal parameters describe the process as physisorption, but applicability of pseudo second order makes it chemisorption. As the rates of reactions are not a good criterion for differentiating between chemisorption and physisorption, the biosorption of Direct Blue 15 dye on fruit-fibers of *Luffa cylindrica* can be described as a physico-chemical process.

Acknowledgement

We are thankful to University of the Punjab for providing research facilities and financial support.

References

- [1] T. Robinson, G. McMullan, R. Marchant, P. Nigam, Remediation of dyes in textile effluent: a critical review on current treatment technologies with a proposed alternative, *Bioresour. Technol.*, 77(3) (2001) 247–255.
- [2] C.J. Ogugbue, T. Sawidis, Bioremediation and detoxification of synthetic wastewater containing triarylmethane dyes by *Aeromonas hydrophila* isolated from industrial effluent, *Biotechnol. Res. Int.*, 2011. Article ID 967925, 11 pages. DOI: 10.4061/2011/967925.
- [3] A.B. Dos Santos, F.J. Cervantes, J.B. van Lier, Review paper on current technologies for decolourisation of textile wastewaters: perspectives for anaerobic biotechnology, *Bioresour. Technol.*, 98(12) (2007) 2369–2385.
- [4] A.M. Talarposhti, T. Donnelly, G.K. Anderson, Colour removal from a simulated dye wastewater using a two-phase anaerobic packed bed reactor, *Water Res.*, 35(2) (2001) 425–432.
- [5] L.K. Lowry, W. Tolos, M.F. Boeniger, C.R. Nony, M.C. Bowman, Chemical monitoring of urine from workers potentially exposed to benzidine-derived azo dyes, *Toxicol. Lett.*, 7(1) (1980) 29–36.
- [6] G. Bayramoğlu, G. Çelik, M.Y. Arica, Biosorption of Reactive Blue 4 dye by native and treated fungus *Phanerocheate chrysosporium*: Batch and continuous flow system studies, *J. Hazard. Mater.*, 137(3) (2006) 1689–1697.
- [7] L.C. Morais, O.M. Freitas, E.P. Goncalves, L.T. Vasconcelos, C.G. Beca, Reactive dyes removal from wastewaters by adsorption on eucalyptus bark: variables that define the process, *Water Res.*, 33(4) (1999) 979–988.
- [8] M.S. Chiou, H.Y. Li, Equilibrium and kinetic modeling of adsorption of reactive dye on cross-linked chitosan beads, *J. Hazard. Mater.*, 93 (2002) 233–248.

- [9] H. Demir, A. Top, D. Balköse, S. Ülkü, Dye adsorption behavior of *Luffa cylindrica* fibers, *J. Hazard. Mater.*, 153 (2008) 389–394.
- [10] S.S. Ahluwalia, D. Goyal, Microbial and plant derived biomass for removal of heavy metals from wastewater, *Bioresour. Technol.*, 98(12) (2007) 2243–2257.
- [11] B. Volesky, Detoxification of metal-bearing effluents: biosorption for the next century, *Hydrometallurgy*, 59(2) (2001) 203–216.
- [12] C. Ye, N. Hu, Z. Wang, Experimental investigation of *Luffa cylindrica* as a natural sorbent material for the removal of a cationic surfactant, *J. Taiwan. Inst. Chem. Eng.*, 44(1) (2013) 74–80.
- [13] B.H. Hameed, M.I. El-Khaiary, Malachite green adsorption by rattan sawdust: isotherm, kinetic and mechanism modeling, *J. Hazard. Mater.*, 159 (2008) 574–579.
- [14] A.S. Alzaydien, Adsorption behavior of methyl orange onto wheat bran: Role of surface and pH, *Oriental J. Chem.*, 31(2) (2015) 643–651.
- [15] P.K. Malik, Use of activated carbons prepared from sawdust and rice-husk for adsorption of acid dyes: a case study of Acid Yellow 36, *Dyes Pigments*, 56(3) (2003) 239–249.
- [16] A.A. Attia, A.N. El-Hendawy, S.A. Khedr, T.H. El-Nabarawy, Textural properties and adsorption of dyes onto carbons derived from cotton stalks, *Adsorpt. Sci. Tech.*, 22(5) (2004) 411–426.
- [17] R. Rehman, T. Mahmud, R. Ejaz, A. Rauf, L. Mitu, Sorptive removal of Direct Blue 15 dye from water using *Camellia sinensis* and *Carica papaya* leaves, *Bulg. Chem. Commun.*, 49(1) (2017) 20–25.
- [18] A.P. Vieira, S.A.A. Santana, C.W.B. Bezerra, H.A.S. Silva, J.A.P. Chaves, J.C.P. Melo, E.C.S. Filho, C. Airold, Kinetics and thermodynamics of textile dye adsorption from aqueous solutions using babassu coconut mesocarp, *J. Hazard. Mater.*, 166 (2009) 1272–1278.
- [19] F. Deniz, S. Karaman, Removal of Basic Red 46 dye from aqueous solution by pine tree leaves, *Chem. Eng. J.*, 170 (2011) 67–74.
- [20] U.S. Orlando, T. Okuda, W. Nishijima, Chemical properties of anion exchangers prepared from waste natural materials, *React. Funct. Polym.*, 55 (2003) 311–318.
- [21] R. Gong, Y. Ding, M. Li, C. Yang, H. Liu, Y. Sun, Utilization of powdered peanut hull as biosorbent for removal of anionic dyes from aqueous solution, *Dyes Pigments*, 64(3) (2005) 187–192.
- [22] G.N. Manju, C. Raji, T.S. Anirudhan, Evaluation of coconut husk carbon for the removal of arsenic from water, *Water Res.*, 32(10) (1998) 3062–3070.
- [23] I.O. Mazali, O.L. Alves, Morphosynthesis: high fidelity inorganic replica of the fibrous network of loofa sponge (*Luffa cylindrica*), *An. Acad. Bras. Ciênc.*, 77(1) (2005) 25–31.
- [24] N. Boudechiche, H. Mokaddem, Z. Sadaoui, M. Trari, Biosorption of cationic dye from aqueous solutions onto lignocellulosic biomass (*Luffa cylindrica*), *Int. J. Indust. Chem.*, 7(2) (2016) 167–180.
- [25] A. Altınışık, E. Gür, Y. Seki, A natural sorbent, *Luffa cylindrica* for the removal of a model basic dye, *J. Hazard. Mater.*, 179(1) (2010) 658–664.
- [26] O.S. Esan, O.N. Abiola, O. Owoyomi, C.O. Aboluwoye, M.O. Osundiya, Adsorption of Brilliant Green onto *Luffa cylindrica* Sponge: Equilibrium, Kinetics, and Thermodynamic Studies, *I.S.R.N. Phys. Chem.*, 2014, Article ID 743532, 12 pages. DOI: 10.1155/2014/743532.
- [27] A. Rauf, T. Mahmud, M. Ashraf, R. Rehman, Sorptive removal of alizarin yellow-R from the water using fibers of *Luffa cylindrica* sponge, *Int. J. Environ. Sustain.*, 12(4) (2016) 31–47.
- [28] M. Iqbal, A. Saeed, Biosorption of reactive dye by loofa sponge-immobilized fungal biomass of *Phanerochaete chrysosporium*, *Process Biochem.*, 42(7) (2007) 1160–1164.
- [29] M.A. Mazmanci, A. Ünyayar, Decolourisation of Reactive Black 5 by *Funalia trogii* immobilised on *Luffa cylindrica* sponge, *Process Biochem.*, 40(1) (2005) 337–342.
- [30] G.D. Saratale, R.G. Saratale, J.S. Chang, S.P. Govindwar, Fixed-bed decolorization of Reactive Blue 172 by *Proteus vulgaris* NCIM-2027 immobilized on *Luffa cylindrica* sponge, *Int. Biodegrad.*, 65(3) (2011) 494–503.
- [31] P. Saueprearsit, M. Nuanjaraen, M. Chinlapa, Biosorption of lead (Pb²⁺) by *Luffa cylindrica* fiber, *Environ. Res. J.*, 4(1) (2010) 157–166.
- [32] I.O. Obboh, E.O. Aluyor, T.O. Audu, Application of *Luffa cylindrica* in natural form as biosorbent to removal of divalent metals from aqueous solutions-kinetic and equilibrium study. In *Waste Water Treatment and Reutilization*, edited by Fernando Sebastián García Einschlag, Carotia: InTech. (2011) 195–213.
- [33] A. Shahidi, N. Jalilnejad, E. Jalilnejad, A study on adsorption of cadmium (II) ions from aqueous solution using *Luffa cylindrica*, *Desal. Water Treat.*, 53(13) (2015) 3570–3579.
- [34] Society of Dyers and Colourists (1971a). *Colour Index* (3rd ed.), Vol. 4, p. 4208, Bradford, Yorkshire.
- [35] K.T. Perez, E.W. Davey, G.E. Morrison, A.W. Super, S. Marino, Environmental assessment of Benzidine based Azo dye, Direct Blue 15 in Experimental Marine Microcosms, U.S. Environmental Protection Agency, ERL-N contribution No. 882 (1987) Narragansett, RI.
- [36] F. Lyon, Occupational exposures of hairdressers and barbers and personal use of hair colourants, some hair dyes, cosmetic colourants, industrial dyestuffs and aromatic amines, *IARC Monographs on the Evaluation of Carcinogenic Risks to Humans*, 57 (1993) 235–245.
- [37] N. Yilgor, C. Köse, E. Terzi, A.K. Figen, R. Ibach, S.N. Kartal, S. Pişkin, Degradation behavior and accelerated weathering of composite boards produced from waste Tetra Pak® packaging materials, *BioResources*, 9(3) (2014) 4784–4807.
- [38] I. Langmuir, The adsorption of gases on plane surfaces of glass, mica and platinum, *J. Am. Chem. Soc.*, 40 (1918) 1361–1403.
- [39] H.M.F. Freundlich, Over the adsorption in solution, *J. Phys. Chem.*, 57 (1906) 385–470.
- [40] M.I. Temkin, V. Pyzhev, Kinetics of ammonia synthesis on promoted iron catalysts, *Acta Physicochim. U. R. S. S.*, 12 (1940) 217–222.
- [41] M.M. Dubinin, L.V. Radushkevich, Equation of the characteristic curve of activated charcoal, *Chem. Zentr.*, 1 (1947) 875–890.
- [42] M.M. Dubinin, The potential theory of adsorption of gases and vapors for adsorbents with energetically non-uniform surface, *Chem. Rev.*, 60 (1960) 235–241.
- [43] D. Ghosh, G.K. Bhattacharyya, Adsorption of methylene blue on kaolinite, *Appl. Clay Sci.*, 20 (2002) 295–300.
- [44] V. Fierro, V. Torné-Fernández, D. Montané, A. Celzard, Adsorption of phenol onto activated carbons having different textural and surface properties, *Micropor. Mesopor. Mater.*, 111(1) (2008) 276–284.
- [45] A.A. Nunes, A.S. Franca, L.S. Oliveira, Activated carbons from waste biomass: an alternative use for biodiesel production solid residues, *Bioresour. Technol.*, 100(5) (2009) 1786–1792.
- [46] M.J. Horsfall, A.I. Spiff, A.A. Abia, Studies on the influence of mercaptoacetic acid (MAA) modification of cassava (manihot sculenta cranz) waste biomass on the adsorption of Cu²⁺ and Cd²⁺ from aqueous solution, *Bullet. Korean Chem. Soc.*, 25(7) (2004) 969–976.
- [47] A.U. Itodo, U.O. Happiness, I.O. Obaroh, A.U. Usman, S.S. Audu, R.D. Temkin, Langmuir and Freundlich adsorption isotherms of industrial dye uptake onto H₃PO₄ catalyzed poultry waste bioadsorbent, *J. Sci. Technol. Res.*, 8(1) (2009) 52–56.
- [48] J.P. Silva, S. Sousa, J. Rodrigues, H. Antunes, J.J. Porter, I. Gonçalves, S. Ferreira-Dias, Adsorption of acid orange 7 dye in aqueous solutions by spent brewery grains, *Sep. Purif. Technol.*, 40(3) (2004) 309–315.
- [49] S. Lagergren, About the theory of so-called adsorption of soluble substances, *Kung. Sven. Vetensk. Handl.*, 24(4) (1898) 1–39.
- [50] Y.S. Ho, G. McKay, Kinetic models for the sorption of dye from aqueous solution by wood, *Process Saf. Environ. Prot.*, 76(2) (1998) 183–191.

- [51] S. Chien, W. Clayton, Application of Elovich equation to the kinetics of phosphate release and sorption in soils, *Soil Sci. Soc. Am. J.*, 44(2) (1980) 265–268.
- [52] A.M. Awwad, N.M. Salem, Kinetics and thermodynamics of Cd(II) biosorption onto loquat (*Eriobotrya japonica*) leaves, *J. Saud. Chem. Soc.*, 18(5) (2014) 486–493.
- [53] G. McKay, Y.S. Ho, J.C.Y. Ng, Biosorption of copper from wastewaters: A review, *Sep. Purif. Methods.*, 28 (1999) 87–125.
- [54] H. Teng, C.T. Hsieh, Activation energy for oxygen chemisorption on carbon at low temperatures, *Indust. Eng. Chem. Res.*, 38(1) (1999) 292–297.
- [55] M.K. Aroua, S.P.P. Leong, L.Y. Teo, C.Y. Yin, W.M.A.W. Daud, Real-time determination of kinetics of adsorption of lead (II) onto palm shell-based activated carbon using ion selective electrode, *Bioresour. Technol.*, 99(13) (2008) 5786–5792.
- [56] G.E. Boyd, A.W. Adamson, L.S. Myers, The exchange adsorption of ions from aqueous solutions on organic zeolites, *Kinetics II*, *J. Am. Chem. Soc.*, 69(11) (1947) 2836–2848.
- [57] W.J. Weber, J.C. Morris, Kinetics of adsorption on carbon from solution, *J. Sanit. Eng. Div. Am. Soc. Civil Eng.*, 89 (1963) 31–60.
- [58] S.J. Allen, G. McKay, K.Y.H. Khader, Intraparticle diffusion of a basic dye during adsorption onto sphagnum peat, *Environ. Pollut.*, 56(1) (1989) 39–50.
- [59] A.E.A.A. Said, A.A. Aly, M.M.A. El-Wahab, S.A. Soliman, A.A.A. El-Hafez, V. Helmey, M.N. Goda, Potential application of propionic acid modified sugarcane bagasse for removing of basic and acid dyes from industrial wastewater, *Resour. Environ.*, 2(3) (2012) 93–99.
- [60] Y.S. Ho, J.C.Y. Ng, G. McKay, Kinetics of pollutant sorption by biosorbents: Review, *Sep. Purif. Methods.*, 29(2) (2010) 189–232.
- [61] J. Sarma, A. Sarma, K.G. Bhattacharyya, Biosorption of commercial dyes on *Azadirachta indica* leaf powder: a case study with a basic dye rhodamine B, *Indust. Eng. Chem. Res.*, 47(15) (2008) 5433–5440.
- [62] T.M. Rao, P.B.R.V. Venkata, Biosorption of Congo Red from aqueous solution by crab shell residue: a comprehensive study, *Springerplus*, 5 (2016) 537.
- [63] M. Solener, S. Tunali, A.S. Ozcan, A. Ozcan, T. Gedikbey, Adsorption characteristics of lead (II) ions onto the clay/poly (methoxyethyl)acrylamide (PMEA) composite from aqueous solutions, *Desalination*, 223 (2008) 308–322.
- [64] F.A. Ugbe, A.A. Pam, A.V. Ikudayisi, Thermodynamic properties of chromium (III) ion adsorption by sweet orange (*Citrus sinensis*) peels, *Am. J. Analyt. Chem.*, 5(10) (2014) 666–673.
- [65] P. Atkins, D.J. Paula, *Atkin's Physical Chemistry*, New York, Oxford University Press, 2010, pp. 894–895.